Institute of Space and Aeronautical Science, University of Tokyo
Report No. 405, August 1966

Supersonic Flow Past Pointed Bodies of Revolution at Small Angles of Attack

By

Keiichi KARASHIMA and Kenjiro IWASAKI*

Summary. A general method of theoretical approach to supersonic flow past lifting bodies of revolution with arbitrary geometry is presented assuming that the flow behind an attached shock wave consists of a basic non-lifting field upon which is superimposed a perturbation field due to small angles of attack and is particularly applied to circular-cones as a simple example.

It is shown that, although the nonlinearity in fundamental equations predicting the basic field has a predominant effect on aerodynamic characteristics of the body, a linear approximation of perturbation field with respect to angle of attack still seems to be available even if the body is not so slender. Experimental results also confirm this.

SYMBOLS

$(\bar{x}, \bar{r}, \theta)$	cylindrical coordinates system
$(\tilde{r}, \phi, \varepsilon)$	polar coordinates system
$\vec{q}$	local velocity vector
$(\bar{u}, \bar{v}, \bar{w})$	components of local velocity vector in cylindrical coordinates system
$(\tilde{u}, \tilde{v}, \tilde{w})$	components of local velocity vector in polar coordinates system
$\bar{p}$	pressure
$\bar{\rho}$	density
$\vec{n}$	unit vector normal to shock wave surface
(x, r, θ)	transformed coordinates system
(u, v, w)	reduced components of local velocity vector
p	reduced pressure
ρ	reduced density
$\bar{a}$	sonic speed
$\bar{c}$	limiting speed
M	free stream Mach number
α	angle of attack
β_s	initial shock wave angle at zero angle of attack
γ	ratio of specific heats

* Mechanical Engineering Research Laboratory, Hitachi Ltd.

δ	semi-vertex angle of cone
ξ	conical variable defined by r/x
ζ	matching parameter of surface entropy
κ	parameter corresponding to deviation of shock wave axis from body axis
$f(\xi)$	component of stream function in basic conical field
$F(\xi)$	density function in basic conical field
$g(\bar{x})$, $h(\bar{x})$	shape functions of shock wave
τ	$\tan \beta_s$
$\omega(x, r, \theta)$	entropy function defined by p/ρ^γ
$\tilde{S}(\bar{x}, \bar{r}, \theta)$	function indicating shock wave surface
S	entropy
c_v	specific heat at constant volume
R	gas constant
Cn_α	slope of normal force coefficient at $\alpha=0°$
Cm_α	slope of pitching-moment coefficient at $\alpha=0°$
Cn	normal force coefficient
Cx	axial force coefficient
Cm	pitching-moment coefficient
Cp	pressure coefficient
$x_{c.p}$	location of center of pressure

SUBSCRIPTS:

o	value in basic field
1	value in perturbation field
∞	value in free stream
s	value at shock wave
e	value at outer edge of vortical layer
c	value at cone surface
t	tangential component to shock wave surface
n	normal component to shock wave surface
$(\ )'$	derivative with respect to argument

1. INTRODUCTION

Among many analytical approaches which have been already developed for lifting bodies of revolution at supersonic speeds, the linearized theory seems to be one of the most well-refined and convenient for many scientific and engineering interests. However, being based upon an assumption of small perturbation, the linearized theory is known to be inaccurate when it is applied to such thick bodies of practical interest, for which the essential feature of flow is nonlinear.

This circumstance required more rigorous methods of analytical approach and several nonlinear theories applied to circular-cones having small angles of attack have been developed by taking entropy change into consideration, since the flow past circular-cones has a simple geometry and a similar exact solution [*1*] at zero angle of attack has already been obtained. For example, by means of the development proposed by Stone [*2*], values of flow properties around circular-cones at an angle of attack were tabulated by Kopal [*3*].

However, Ferri [*4*] pointed out that the existence of a singular point at the cone surface is neglected in references [*2*] and [*3*] and, consequently, an erroneous distribution of entropy at the cone surface is obtained. He tried to treat this singular point by introducing a concept of a vortical layer next to the cone surface and showed that the Kopal's tables can be used if a simple correction is introduced. Later, Sims [*5*] presented a detailed chart of tables of flow properties around right circular-cones at small angles of attack. The results contained in these tables were computed in the same basic manner as those of reference [*3*] with the correct velocity normal to meridian planes.

Ferri further presented a series of papers [*6*], [*7*], [*8*] concerning a general method of numerical approach to supersonic flow past lifting bodies of revolution. This method is developed by use of an intrinsic coordinates system and is called as 'linearized characteristics method'. Recently, Rakich [*9*] obtained numerical solutions of supersonic flow past blunt cones and ogival bodies of revolution at small angles of attack by using the linearized characteristics method to continue the blunt body solutions proposed by Van Dyke and Gordon [*10*] to supersonic region.

These methods are based upon an assumption that the physical properties in flow field can be developed in Fourier series in terms of the angle of attack. From experimental point of view, this assumption seems to be reasonable for small angles attack even in case that the body is comparatively thick.

In this paper, a general method of analytical approach to supersonic flow past pointed bodies of revolution at small angles of attack. Although the same assumption as was made in existing works is used in development of flow properties, the present approach has a different procedure for determining the flow around pointed bodies at small angles of attack in a sense that it can be obtained as a result of an extension of the analytical approach to axially symmetric supersonic flows proposed by Karashima [*11*] to lifting problems. The values obtained in this way are compared with experimental results at several values of angle of attack.

2. Fundamental Equations

Let the origin of a cylindrical coordinates system $(\bar{x}, \bar{r}, \theta)$ be taken at the vertex of the body, $\bar{x}$-axis being aligned with the body axis (see Fig. 1a). The continuity equation, three momentum equations and entropy equation are expressed, respectively, as

$$(\bar{\rho}\bar{u}\bar{r})_{\bar{x}}+(\bar{\rho}\bar{v}\bar{r})_{\bar{r}}+(\bar{\rho}\bar{w})_{\theta}=0, \tag{2.1a}$$

$$\bar{u}\bar{u}_{\bar{x}}+\bar{v}\bar{u}_{\bar{r}}+\frac{\bar{w}}{\bar{r}}\bar{u}_{\theta}+\frac{1}{\bar{\rho}}\bar{p}_{\bar{x}}=0, \tag{2.1b}$$

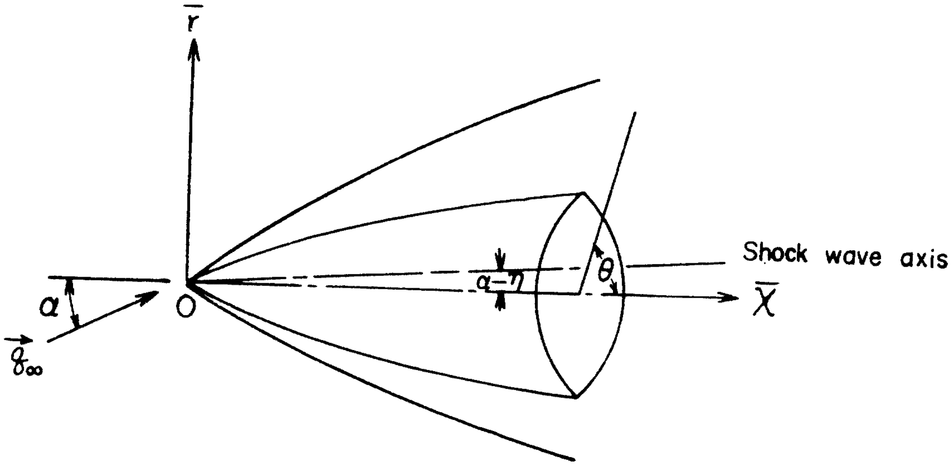

FIG. 1a. Cylindrical coordinates system.

$$\bar{u}\bar{v}_{\bar{x}}+\bar{v}\bar{v}_{\bar{r}}+\frac{\bar{w}}{\bar{r}}\bar{v}_\theta-\frac{\bar{w}^2}{\bar{r}}+\frac{1}{\bar{\rho}}\bar{p}_{\bar{r}}=0, \tag{2.1c}$$

$$\bar{u}\bar{w}_{\bar{x}}+\bar{v}\bar{w}_{\bar{r}}+\frac{\bar{w}}{\bar{r}}\bar{w}+\frac{\bar{v}\bar{w}}{\bar{r}}+\frac{1}{\bar{r}\bar{\rho}}\bar{p}_\theta=0, \tag{2.1d}$$

$$\bar{v}\bar{\omega}_{\bar{x}}+\bar{v}\bar{\omega}_{\bar{r}}+\frac{\bar{w}}{\bar{r}}\bar{\omega}_\theta=0, \quad \bar{\omega}=\bar{p}/\bar{\rho}^\gamma. \tag{2.1e}$$

Introducing a transformation of variable such as

$$x=\bar{x}, \quad r=\frac{1}{\tau}\bar{r}, \quad \tau=\tan\beta_s, \tag{2.2}$$

$$\left.\begin{aligned}
&\bar{u}=\bar{q}_\infty\{\tilde{a}+\tau^2u(x,r,\theta)\}, \quad \tilde{a}=1+\frac{2}{(\gamma+1)M^2},\\
&\bar{v}=\bar{q}_\infty\tau v(x,r,\theta),\\
&\bar{w}=\bar{q}_\infty\tau w(x,r,\theta),\\
&\bar{\rho}=\bar{\rho}_\infty\rho(x,r,\theta),\\
&\bar{p}=\bar{p}_\infty\gamma M^2\tau^2p(x,r,\theta),
\end{aligned}\right\} \tag{2.3}$$

and rewriting Eq. (2.1), then, yields

$$\{r\rho(\tilde{a}+\tau^2u)\}_x+(r\rho v)_r+(\rho w)_\theta=0, \tag{2.4a}$$

$$(\tilde{a}+\tau^2u)u_x+vu_r+\frac{w}{r}u_\theta+\frac{1}{\rho}p_x=0, \tag{2.4b}$$

$$(\tilde{a}+\tau^2u)v_x+vv_r+\frac{w}{r}v_\theta-\frac{w^2}{r}+\frac{1}{\rho}p_r=0, \tag{2.4c}$$

$$(\tilde{a}+\tau^2u)w_x+vw_r+\frac{w}{r}w_\theta+\frac{vw}{r}+\frac{1}{r\rho}p_\theta=0, \tag{2.4d}$$

$$(\tilde{a}+\tau^2u)\omega_x+v\omega_r+\frac{w}{r}\omega_\theta=0, \quad \omega=p/\rho^\gamma. \tag{2.4e}$$

If the body is at a small angle of attack, flow field down-stream of an attached shock wave can be considered to consist of a basic field corresponding to zero angle of attack upon which is superimposed a perturbation field due to the incidence. Therefore, it will be reasonable to assume that physical properties in the disturbed field have the forms, as a first-order approximation, as

$$\left.\begin{aligned} u(x,r,\theta)&=u_0(x,r)+\alpha u_1(x,r)\sin\theta,\\ v(x,r,\theta)&=v_0(x,r)+\alpha v_1(x,r)\sin\theta,\\ w(x,r,\theta)&=\alpha w_1(x,r)\cos\theta,\\ \rho(x,r,\theta)&=\rho_0(x,r)+\alpha\rho_1(x,r)\sin\theta,\\ p(x,r,\theta)&=p_0(x,r)+\alpha p_1(x,r)\sin\theta. \end{aligned}\right\} \tag{2.5}$$

Substitution of Eq. (2.5) into Eq. (2.4) and equating like powers of α yields simultaneous equations concerning the basic field and perturbation field, respectively. The equations for the basic field can be written as

$$\left.\begin{aligned} &\{r\rho_0(\tilde{a}+\tau^2u_0)\}_x+(r\rho_0v_0)_r=0,\\ &(\tilde{a}+\tau^2u_0)u_{ox}+v_ou_{or}+\frac{1}{\rho_0}p_{ox}=0,\\ &(\tilde{a}+\tau^2u_0)v_{ox}+v_ov_{or}+\frac{1}{\rho_0}p_{or}=0,\\ &(\tilde{a}+\tau^2u_0)\omega_{ox}+v_0\omega_{or}=0,\qquad \omega_0=p_0/\rho_0^{\gamma}. \end{aligned}\right\} \tag{2.6}$$

It is clear that Eq. (2.6) is the fundamental equations for axially symmetric flow and the solution can be obtained by use of the method proposed by Karashima [*11*].

The simultaneous equations for perturbation field of the first-order are given as

$$\left.\begin{aligned} &\{r\rho_1(\tilde{a}+\tau^2u_0)\}_x+(r\rho_0u_1)_x+(r\rho_1v_0)_r+(r\rho_0v_1)_r-\rho_0w_1=0,\\ &(\tilde{a}+\tau^2u_0)u_{1x}+\tau^2u_{ox}u_1+v_0u_{1r}+u_{or}v_1+\frac{p_{1x}}{\rho_0}-\frac{\rho_1p_{ox}}{\rho_0^2}=0,\\ &(\tilde{a}+\tau^2u_0)v_{1x}+\tau^2v_{ox}u_1+v_0v_{1r}+v_{or}v_1+\frac{p_{1r}}{\rho_0}-\frac{\rho_1p_{or}}{\rho_0^2}=0,\\ &(\tilde{a}+\tau^2u_0)w_{1x}+v_0w_{1r}+\frac{v_0w_1}{r}+\frac{p_1}{r\rho_0}=0,\\ &(\tilde{a}+\tau^2u_0)\omega_{1x}+\tau^2\omega_{or}u_1+v_0\omega_{1r}+\omega_{or}v_1=0,\\ &\omega_1=\frac{p_1}{\rho_0^{\gamma}}-\frac{\gamma p_0\rho_1}{\rho_0^{\gamma+1}}. \end{aligned}\right\} \tag{2.7}$$

3. Generalized Boundary Conditions

The conditions across an attached shock wave can be divided into two parts. The one is conservation of tangential velocity component and the another is jump conditions of flow properties normal to the shock wave surface. If the shock wave surface is given by the equation

$$\tilde{S}(\bar{x}, \bar{r}, \theta)=0, \tag{3.1}$$

then, generalized shock wave conditions can be written as
(tangential condition)

$$\vec{q}_{\infty t}=\vec{q}_{st}, \tag{3.2}$$

(normal conditions)

$$\vec{q}_{\infty n}=\frac{1}{\Gamma}\vec{q}_{ns}, \tag{3.3}$$

$$\frac{\bar{\rho}_s}{\bar{\rho}_\infty}=\frac{(\gamma+1)\left(\dfrac{\vec{n}\cdot\vec{q}_\infty}{a_\infty}\right)^2}{(\gamma-1)\left(\dfrac{\vec{n}\cdot\vec{q}_\infty}{a_\infty}\right)^2+2}=\frac{1}{\Gamma}, \tag{3.4}$$

$$\frac{\bar{p}_s}{\bar{p}_\infty}=1+\frac{2\gamma}{\gamma+1}\left\{\left(\frac{\vec{n}\cdot\vec{q}_\infty}{a_\infty}\right)^2-1\right\}, \tag{3.5}$$

where unit vector normal to shock wave surface, $\vec{n}$, is defined by the equation

$$\vec{n}=\frac{\nabla\tilde{S}}{|\nabla\tilde{S}|}. \tag{3.6}$$

By use of relations

$$\left.\begin{aligned}&\vec{q}_t=(\vec{n}\times\vec{q})\times\vec{n}=\vec{q}-\vec{n}(\vec{n}\cdot\vec{q}),\\&\vec{q}_n=\vec{n}(\vec{n}\cdot\vec{q}),\end{aligned}\right\} \tag{3.7}$$

velocity vector just downstream of shock wave can be expressed as

$$\begin{aligned}\vec{q}_s&=\vec{q}_{ts}+\vec{q}_{ns}\\&=\vec{q}_\infty-(1-\Gamma)\vec{n}(\vec{n}\cdot\vec{q}_\infty).\end{aligned} \tag{3.8}$$

On the other hand, since velocity components in free stream are given by

$$\left.\begin{aligned}&\bar{u}_\infty=\bar{q}_\infty\cos\alpha,\\&\bar{v}_\infty=\bar{q}_\infty\sin\alpha\sin\theta,\\&\bar{w}_\infty=\bar{q}_\infty\sin\alpha\cos\theta,\\&\bar{q}_\infty=|\vec{q}_\infty|,\end{aligned}\right\} \tag{3.9}$$

velocity components just behind the shock wave can be obtained by use of Eqs. (3.8) and (3.9) as

$$\left.\begin{aligned}&\frac{\bar{u}_s}{\bar{q}_\infty}=\cos\alpha-(1-\Gamma)\tilde{\varepsilon}\tilde{S}_{\bar{x}},\\&\frac{\bar{v}_s}{\bar{q}_\infty}=\sin\alpha\sin\theta-(1-\Gamma)\tilde{\varepsilon}\tilde{S}_{\bar{r}},\end{aligned}\right\} \tag{3.10}$$

$$\frac{\bar{w}_s}{\bar{q}_\infty}=\sin\alpha\cos\theta-(1-\Gamma)\tilde{\varepsilon}\frac{1}{\bar{r}}\tilde{S}_\theta,$$

where

$$\tilde{\varepsilon}=\frac{1}{|\nabla\tilde{S}|^2}\left\{\tilde{S}_{\bar{x}}\cos\alpha+\tilde{S}_{\bar{r}}\sin\alpha\sin\theta+\frac{1}{\bar{r}_s}\tilde{S}_\theta\sin\alpha\cos\theta\right\}. \tag{3.11}$$

If the first-order shock wave shape is assumed to have a form

$$\bar{r}_s=g(\bar{x})+\alpha h(\bar{x})\sin\theta, \tag{3.12}$$

then, the shock wave conditions are given, neglecting the terms of order of α^2, as

$$\begin{aligned}
\frac{\bar{u}_s}{\bar{q}_\infty}&=1+\frac{2}{(\gamma+1)M^2}-\frac{2g'^2}{(\gamma+1)(1+g'^2)}\\
&\quad-\alpha\sin\theta\frac{2g'\{M^2g'^2-(1+g'^2)\}}{(\gamma+1)M^2g'^2(1+g'^2)}\left[\frac{2h'-(1+g'^2)}{1+g'^2}+\frac{2\{h'-(1+g'^2)\}}{M^2g'^2-(1+g'^2)}\right],\\
\frac{\bar{v}_s}{\bar{q}_\infty}&=\frac{2}{\gamma+1}\frac{g'}{1+g'^2}\left(1-\frac{1+g'^2}{M^2g'^2}\right)\\
&\quad+\alpha\sin\theta\left[1-\frac{2\{M^2g'^2-(1+g'^2\}}{(\gamma+1)M^2g'^2(1+g'^2)}\left\{\frac{(1-g'^2)h'-(1+g'^2)}{1+g'^2}\right.\right.\\
&\qquad\left.\left.+\frac{2\{h'-(1+g'^2)\}}{M^2g'^2-(1+g'^2)}\right]\right.,\\
\frac{\bar{w}_s}{\bar{q}_\infty}&=\alpha\cos\theta\left[1-\frac{h}{g}\frac{2g'\{M^2g'^2-(1+g'^2)\}}{(\gamma+1)M^2g'^2(1+g'^2)}\right],\\
\frac{\bar{\rho}_s}{\bar{\rho}_\infty}&=\frac{(\gamma+1)M^2g'^2}{(\gamma-1)M^2g'^2+2(1+g'^2)}\left[1+4\alpha\sin\theta\frac{h'-(1+g'^2)}{g'\{(\gamma-1)M^2g'^2+2(1+g'^2)\}}\right],\\
\frac{\bar{p}_s}{\bar{p}_\infty}&=\frac{2\gamma M^2g'^2-(\gamma-1)(1+g'^2)}{(\gamma+1)(1+g'^2)}+4\alpha\sin\theta\frac{\gamma M^2g'^2\{h'-(1+g'^2)\}}{(\gamma+1)g'(1+g'^2)^2}.
\end{aligned} \tag{3.13}$$

It remains to discuss the condition on body surface. If the body surface is given by the equation

$$B(\bar{x},\bar{r})=0, \tag{3.14}$$

tangency condition along the body surface is expressed as

$$\vec{q}\cdot\operatorname{grad}B=0,$$

which can be interpretted into

$$\bar{v}_b=-\bar{u}_bB_{\bar{x}}/B_{\bar{r}}\quad\text{at}\quad B=0, \tag{3.15}$$

where subscript b denotes conditions on body surface.

4. Application to Circular-Cones

As a simple example, consider a supersonic flow past a circular-cone at small angles of attack. In this case, it has been already found that the flow field can be assumed to be conical without axial symmetry. Therefore, the shock wave shape can be assumed to have a simple form

$$\bar{r}_s=\tau\bar{x}(1+\kappa\alpha\sin\theta), \tag{4.1}$$

where κ is an unknown constant to be determined from given boundary conditions. κ has a physical meaning that shock wave axis deviates from body axis due to an angle of attack and the deviation is proportional to $\alpha\kappa$. Since the basic field is conical with axial symmetry and isentropic, an exact similar solution exists. Detailed discussion on this similar solution appropriate to basic conical field was made by Karashima [11] in a different sense from Taylor-Maccoll's conical theory [1] by introducing a conical variable ξ, a stream function ψ and a density function F such as

$$\begin{gathered}\bar{r}_s=g(\bar{x})=\tau\bar{x}, \qquad \xi=\frac{x}{r},\\ \psi(x,r)=x^2f(\xi) \qquad \rho(x,r)=F(\xi),\\ \omega_0=\text{const.}=\frac{2\gamma M^2\tau^2-(\gamma-1)(1+\tau^2)}{\gamma(\gamma+1)M^2\tau^2(1+\tau^2)}\left\{\frac{(\gamma-1)M^2\tau^2+2(1+\tau^2)}{(\gamma+1)M^2\tau^2}\right\}^{\gamma},\end{gathered} \tag{4.2}$$

and, hence,

$$\left.\begin{aligned}\tilde{\alpha}+\tau^2u_0(x,r)&=\frac{f'}{\xi F},\\ v_0(x,r)&=-\frac{2f-\xi f'}{\xi F}.\end{aligned}\right\} \tag{4.3}$$

By use of these relations, Eq. (2.6) can be written as

$$\left.\begin{aligned}&4f^2f''-2ff'^2=\gamma\omega_0\xi^2F^{\gamma}F'\{f'-\tau^2\xi(2f-\xi f')\},\\ &f'^2+\tau^2(2f-\xi f')^2+\frac{2\gamma}{\gamma-1}\tau^2\omega_0\xi^2F^{\gamma+1}=K\xi^2F^2,\end{aligned}\right\} \tag{4.4}$$

where $K=1+\dfrac{2}{(\gamma-1)M^2}$, and the shock wave conditions are obtained from Eq. (3.13) as

$$\left.\begin{aligned}f(1)&=\frac{1}{2},\\ f'(1)&=\frac{\tau^2}{1+\tau^2}\,\frac{\{(\gamma+1)+(\gamma-1)\tau^2\}M^2+2(1+\tau^2)}{(\gamma-1)M^2\tau^2+2(1+\tau^2)},\\ F(1)&=\frac{(\gamma+1)M^2\tau^2}{(\gamma-1)M^2\tau^2+2(1+\tau^2)}.\end{aligned}\right\} \tag{4.5}$$

Another condition is that the stream function vanishes on the cone surface $\xi=\xi_c$. Hence,

$$f(\xi_c)=0. \tag{4.6}$$

Thus, semi-vertex of the cone, δ, is obtained by the relation

$$\tan\delta=\tau\xi_c. \tag{4.7}$$

Substitution of Eq. (4.3) into Eq. (2.7) and rewriting the equations by use of conical variable leads to the following linear simultaneous equations for the perturbation field;

$$\begin{aligned}
&2fF\rho_1'-2fF'\rho_1+\tau^2\xi^2F^2(Fu_1)'-\xi F^3v_1'-F^2(F+\xi F')v_1+F^3w_1=0,\\
&2\tau^2\xi fFu_1'+\tau^2\xi\{\xi Ff''-f'(F+\xi F')\}u_1-\{\xi Ff''-f'(F+\xi F')\}v_1\\
&\qquad\qquad+\tau^2\xi^3Fp_1'-\tau^2\gamma\omega_0\xi^3F^{\gamma-1}F'\rho_1=0,\\
&2\xi fFv_1'+\{\xi F(f'-\xi f'')-(2f-\xi f')(F+\xi F')\}v_1\\
&\qquad-\tau^2\xi\{\xi F(f'-\xi f'')-(2f-\xi f')(F+\xi F')\}u_1\\
&\qquad\qquad-\xi^2Fp_1'+\gamma\omega_0\xi^2F^{\gamma-1}F'\rho_1=0,\\
&2\xi fw_1'+(2f-\xi f')w_1-\xi p_1=0,\\
&Fp_1'-\gamma F'p_1-\gamma\omega_0F^{\gamma-1}(F\rho_1'-F'\rho_1)=0.
\end{aligned} \tag{4.8}$$

Shock wave conditions appropriate to perturbation field can be obtained from Eqs. (3.13) and (4.1) as

$$\begin{aligned}
u_1(1)&=\frac{2\{M^2\tau^2+(1+\tau^2)\}}{(\gamma+1)M^2\tau^3(1+\tau^2)}-\kappa\left\{\frac{4}{(\gamma+1)(1+\tau^2)^2}+u_0'(1)\right\}\\
v_1(1)&=\frac{(\gamma-1)M^2\tau^2+(\gamma+1)M^2\tau^4-2(1+\tau^2)}{(\gamma+1)M^2\tau^3(1+\tau^2)}\\
&\quad+\kappa\left\{2\frac{M^2\tau^2(1-\tau^2)+(1+\tau^2)^2}{(\gamma+1)M^2\tau^2(1+\tau^2)^2}-v_0'(1)\right\},\\
w_1(1)&=\frac{1}{\tau}-\kappa\frac{2\{M^2\tau^2-(1+\tau^2)\}}{(\gamma+1)M^2\tau^2(1+\tau^2)},\\
\rho_1(1)&=-\frac{4(\gamma+1)M^2\tau(1+\tau^2)}{\{(\gamma-1)M^2\tau^2+2(1+\tau^2)\}^2}\\
&\quad+\kappa\left\{\frac{4(\gamma+1)M^2\tau^2}{[(\gamma-1)M^2\tau^2+2(1+\tau^2)]^2}-\rho_0'(1)\right\},\\
p_1(1)&=-\frac{4}{(\gamma+1)\tau(1+\tau^2)}+\kappa\left\{\frac{4}{(\gamma+1)(1+\tau^2)^2}-p_0'(1)\right\}.
\end{aligned} \tag{4.9}$$

It remains to determine the unknown constant κ. It can be so determined as to satisfy the tangency condition, Eq. (3.15), that is

$$v_1(\xi_c;\kappa)=\tau^2\xi_cu_1(\xi_c;\kappa). \tag{4.10}$$

5. Discussion on Discontinuity of Entropy at Cone Surface

In the last section, fundamental equations and boundary conditions appropriate to supersonic flow past circular-cones at small angles of attack have been derived approximately by assuming a conical field without axial symmetry and by neglecting the terms of order of α^2. However, as has been already pointed out by Ferri [4], such a development as is made in the present approach results in a discontinuous distribution of entropy near the cone surface, which can be shown by the following procedure.

Rewriting Eq. (2.4e) by use of conical variable, then, gives

$$\{v-\xi(\tilde{a}+\tau^2 u)\}\,\omega_\xi+\frac{w}{\xi}\,\omega_\theta=0. \tag{5.1}$$

Since the first term of the above equation vanishes at the cone surface (tangency condition), it is easily known that ω_θ must be zero there because of $w\neq 0$. This means that surface entropy must be constant, that is

$$\omega(\xi_c,\theta)=\text{const.} \tag{5.2}$$

On the other hand, the final equation in Eq. (2.7) is clearly obtained by assuming that ω_ξ is of order of α^2 in the whole flow field and, consequently, negligible,

$$\omega_\xi=0. \tag{5.3}$$

This means that entropy in each meridian plane remains constant. However, since the cone is at an angle of attack, the axis of conical shock wave does no longer remain coincident with the direction of free stream velocity vector and, therefore, entropy function just behind the shock wave must have a form

$$\omega(1,\theta)=\omega_0+\alpha\omega_1(1)\sin\theta,$$

where

$$\left.\begin{aligned}&\omega_0=\text{const.}\\&\omega_1=\omega_1(1)=\omega_0\left\{\frac{p_1(1)}{p_0(1)}-\gamma\frac{\rho_1(1)}{\rho_0(1)}\right\}.\end{aligned}\right\} \tag{5.4}$$

From the assumption denoted by Eq. (5.3), surface entropy is given by the equation

$$\omega(\xi_c,\theta)=\omega_0+\alpha\omega_1\sin\theta, \tag{5.5}$$

which is obviously a function of θ. Therefore, if ω_1 is of order of unity, there arises a contradiction between Eqs. (5.2) and (5.3).

The inconsistency in entropy distribution is clearly due to the assumption of conical field without axial symmetry and also to the prediction of perturbation of flow quantities such as given by Eq. (2.5). In order to examine this circumstance in more detail, consider a polar coordinates system $(\tilde{r},\phi,\varepsilon)$ (see Fig. 1b) with its origin coincident with vertex of the cone. Then, continuity equation can be written

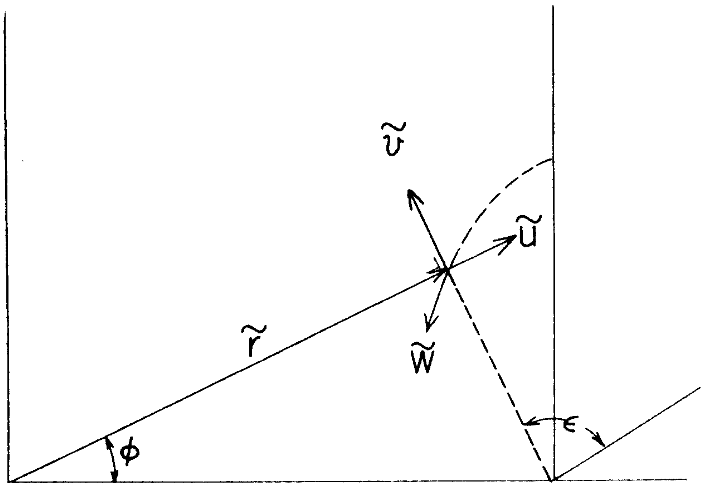

FIG. 1b. Polar coordinates system.

by use of the assumption of conical field as

$$\tilde{v}\frac{\partial\tilde{u}}{\partial\phi}+\frac{\tilde{w}}{\sin\phi}\frac{\partial\tilde{u}}{\partial\varepsilon}-\tilde{v}^2-\tilde{w}^2=0, \tag{5.6}$$

where $(\tilde{u}, \tilde{v}, \tilde{w})$ denotes velocity components in this coordinates system. If velocity components are assumed to have forms

$$\left.\begin{aligned}\tilde{u}(\tilde{r}, \phi, \varepsilon)&=\tilde{u}_0(\tilde{r}, \phi)+\alpha\tilde{u}_1(\tilde{r}, \phi)\sin\varepsilon,\\ \tilde{v}(\tilde{r}, \phi, \varepsilon)&=\tilde{v}_0(\tilde{r}, \phi)+\alpha\tilde{v}_1(\tilde{r}, \phi)\sin\varepsilon,\\ \tilde{w}(\tilde{r}, \phi, \varepsilon)&=\qquad\qquad\ \ \alpha\tilde{w}_1(\tilde{r}, \phi)\cos\varepsilon,\end{aligned}\right\} \tag{5.7}$$

the following relations can be obtained from the continuity equation by neglecting the terme of order of α^2,

$$\left.\begin{aligned}&\frac{\partial\tilde{u}_0}{\partial\phi}-\tilde{v}_0=0,\\ &\frac{\partial\tilde{u}_1}{\partial\phi}-\tilde{v}_1=0,\end{aligned}\right\} \tag{5.8}$$

On the other hand, since vorticity components in the disturbed flow field can be expressed, respectively, by use of Eq. (5.7) as

$$\text{rot}_{\tilde{r}}\vec{q}=\frac{\alpha\cos\varepsilon}{\tilde{r}\sin\phi}\left(\tilde{w}_1\cos\phi+\sin\phi\frac{\partial\tilde{w}_1}{\partial\phi}-\tilde{v}_1\right), \tag{5.9a}$$

$$\text{rot}_{\phi}\vec{q}=\frac{\alpha\cos\varepsilon}{\tilde{r}}\left(\frac{\tilde{u}_1}{\sin\phi}-\tilde{w}_1\right), \tag{5.9b}$$

$$\text{rot}_{\varepsilon}\vec{q}=\frac{1}{\tilde{r}}\left\{\left(\tilde{v}_0-\frac{\partial\tilde{u}_0}{\partial\phi}\right)+\alpha\sin\varepsilon\left(\tilde{v}_1-\frac{\partial\tilde{u}_1}{\partial\phi}\right)\right\}, \tag{5.9c}$$

it is easily found from Eq. (5.8) that $\text{rot}_{\varepsilon}\vec{q}$ is of order of α^2 and, hence, negligible, that is

$$\mathrm{rot}_\varepsilon \vec{q} = 0 .$$

Moreover, it follows from Crocco's vortex law,

$$\vec{q} \times \mathrm{rot}\, \vec{q} = -\mathrm{Tgrad}\, S, \tag{5.10}$$

that $\mathrm{rot}_\phi \vec{q}$ is also of order of α^2 and negligible from the assumption, where T denotes temperature and S is entropy. This, in turn, gives a relation

$$\tilde{u}_1 = \tilde{w}_1 \cos \phi .$$

Differentiation of the above equation with respect to ϕ and substituting it into Eq. (5.9a) leads to a result that $\mathrm{rot}_\tau \vec{q}$ also vanishes. Hence,

$$\mathrm{rot}\, \vec{q} = 0 . \tag{5.11}$$

As can be seen from Eq. (5.10), this result clearly indicates a remarkable fact that the assumptions made in the present development is essentially consistent with an assumption of isentropic flow everywhere in the disturbed field, which contradicts the azimuthal distribution of entropy aft of the shock wave, if ω_1 is of order of unity. Because of this circumstance, validity of the present approach seems to depend mainly upon the order of magnitude of ω_1.

Substitution of Eq. (4.9) into Eq. (5.4) gives

$$\omega_1 = 4\omega_0 \left(\kappa - \frac{1+\tau^2}{\tau}\right) \frac{\gamma(\gamma-1)\{M^2\tau^2-(1+\tau^2)\}^2}{(1+\tau^2)\{2\gamma M^2\tau^2-(\gamma-1)(1+\tau^2)\}\{(\gamma-1)M^2\tau^2+2(1+\tau^2)\}} . \tag{5.12}$$

Since the term $\{M^2\tau^2-(1+\tau^2)\}$ is of order of δ, ω_1 must be of order of δ^2. Therefore, the isentropic assumption consistent with the present development can be approximately satisfied, if δ is small so that

$$\alpha\delta^2 \ll 1 . \tag{5.13}$$

However, it must be noted that, irrespective of an additional condition given by Eq. (5.13), the assumption denoted by Eq. (5.3) seems to be applicable near the shock wave even in case of a large cone angle, since both $\overline{w}$ and $\overline{\omega}_\theta$ are of order of α there. This fact leads to a statement that entropy in each meridian plane is approximately constant near the shock wave and most of entropy increase which is of order of α occurs near the cone surface. This implicitly suggests that the present development may be further applicable to a cone with comparatively large semi-vertex angle by introducing a suitable correction of entropy distribution near the surface. Thus, it becomes of primary interest to inquire the region in which an abrupt entropy change takes place.

For this purpose is to be introduced a replacement

$$v_n = v - \xi(\tilde{a} + \tau^2 u), \tag{5.14}$$

which corresponds to velocity component normal to each ray from the origin ($\tilde{r}$ in polar coordinates system). Since v_n must vanish at the cone surface $\xi=\xi_c$, Eq. (5.14) can be expressed near the surface as

$$v_n \doteqdot A(\xi-\xi_c),$$

where A is a constant of order of unity. In the region where v_n is of order of unity ω_ξ is of order of α^2 and the entropy change in this region is of order of α^2. Near the surface where $(\xi-\xi_c)$ is of order of α, v_n also tends to be order of α. Although ω_ξ may become of order of α in this region, corresponding entropy increase must be of order of α^2 and, therefore, negligible from the assumption, since thickness of this region is of order of α. These results explicitly suggest that an abrupt entropy increase of order of α must take place in a layer of thickness of order of α^2 next to the cone surface where v_n tends to be of order of α^2. This layer was called the vortical layer by Ferri [4], in which vorticity cannot be neglected. The axis of vortex can be easily shown to align with meridian line of the cone.

The appearance of thin vortical layer next to the cone at small angles of attack can be recognized as follows. Since v_n is always negative, all streamlines that start at the shock wave approach the cone surface as they flow downstream. Near the shock wave azimuthal displacement of the streamlines is very small because of $v_n \sim 0(1)$ and $w \sim 0(\alpha)$, and entropy change in this region is, therefore, of order of α^2. Near the cone surface v_n becomes very small, so that streamlines tend to be parallel to the surface because of cross flow w. Moreover, since $w=0$ in meridian planes $\theta=\pm\pi/2$ and $w>0$ in $-\pi/2<\theta<\pi/2$, projection of streamlines near the cone surface to a spherical surface $\tilde{r}=$const. tends to diverge at $\theta=-\pi/2$ and converge at $\theta=\pi/2$. This converging characteristic of streamline projections with different entropy level into a thin layer next to the cone surface (vortical layer) causes, therefore, an abrupt gradient of entropy normal to the cone.

Consider a vortical layer of infinitesimal thickness next to a cone at small angles of attack, across which flow properties change abruptly. The conditions at outer edge of the vortical layer, which is denoted by a subscript e, are assumed to be given by the solutions of equations formulated in Section 4. Because of $w=0$ in meridian plane $\theta=-\pi/2$, streamlines entering this plane through shock wave remain in the same plane. Furthermore, since there is no singularity in this plane, it will be reasonable to assume that surface entropy has the same value that is given in this plane, that is

$$S_c=S_0-\alpha S_1, \tag{5.15}$$

where

$$\left.\begin{aligned} S_0&=S_\infty+c_v\log\gamma M^2\tau^2\omega_0, \\ S_1&=c_v\omega_1/\omega_0. \end{aligned}\right\} \tag{5.16}$$

This assumption clearly indicates that flow phenomena can be represented by the equations predicted in Section 4, where entropy remains constant until a vortical layer of infinitesimal thickness is reached at the cone surface across which an abrupt variation of entropy takes place from the value $S_0+\alpha S_1\sin\theta$ to the value $S_0-\alpha S_1$ that exists at the surface. Thus, increase of entropy across the vortical layer is given by

$$\varDelta S=S_c-S_e=-\alpha S_1(1+\sin\theta). \tag{5.17}$$

By combining an isoenergetic equation with an entropy equation

$$\left.\begin{aligned}\frac{1}{\bar\rho}\bar p_\theta-\frac{\bar p}{\bar\rho^2}\bar\rho_\theta&=-\frac{\gamma-1}{\gamma}(\bar u\bar u_\theta+\bar v\bar v_\theta+\bar w\bar w_\theta),\\ \frac{\gamma-1}{R}S_\theta&=\frac{1}{\bar p}\bar p_\theta-\frac{\gamma}{\bar\rho}\bar\rho_\theta,\end{aligned}\right\} \tag{5.18}$$

and further by introducing the tangential condition, $\bar v_c=\xi_c\bar u_c$, a velocity relation available at the cone surface is obtained as

$$\bar v_c\bar w_c=\bar u_c\left(\frac{\partial\bar u}{\partial\theta}\right)_c+\bar v_c\left(\frac{\partial\bar v}{\partial\theta}\right)_c,$$

and this equation is further simplified by introducing Eqs. (2.3) and (2.5) into following two relations;

$$\left.\begin{aligned}v_{0c}w_{1c}&=(\tilde a+\tau^2u_{0c})u_{1c}+v_{0c}v_{1c},\\ v_{1c}w_{1c}&=\tau^2u_{1c}^2+v_{1c}^2.\end{aligned}\right\} \tag{5.19}$$

However, these two equations are easily shown to be consistent with one another by substituting the tangential conditions

$$\begin{aligned}v_{0c}&=\xi_c(\tilde a+\tau^2u_{0c}),\\ v_{1c}&=\tau^2\xi_cu_{1c}.\end{aligned}$$

Therefore, cross flow component along the cone surface is obtained from Eq. (5.19) as

$$w_{1c}=\frac{1+\tau^2\xi_c^2}{\xi_c}u_{1c}. \tag{5.20}$$

On the other hand, since thickness of the vortical layer is of order of α^2 and must be thinner to vanish as angle of attack approaches zero, it will be reasonable to assume that

$$\left.\begin{aligned}u_{1c}&=\zeta u_{1e},\\ v_{1c}&=\zeta v_{1e},\end{aligned}\right\} \tag{5.21}$$

where ζ is an unknown constant to be determined from matching of entropy across the vortical layer. It is convenient to see that the assumption denoted by Eq. (5.21) does not disturb the tangential condition for perturbation field and, consequently, the unknown constant involved in shock wave conditions can be determined from the relation

$$v_{1e}(\xi_c;\kappa)=\tau^2\xi_c u_{1e}(\xi_c;\kappa). \tag{5.22}$$

Pressure ratio across the vortical layer being given by the equation

$$\frac{p_c}{p_e}=\left(\frac{\bar{c}^2-\bar{q}_c^{\,2}}{\bar{c}^2-\bar{q}_e^{\,2}}\right)^{\frac{\gamma}{\gamma-1}}e^{-\frac{\Delta S}{(\gamma-1)Cv}}, \tag{5.23}$$

it can be easily found that surface pressure consistent with the entropy increase such as given by Eq. (5.17) must have a form

$$p_c=p_0+\alpha(\tilde{p}+p_{1e}\sin\theta), \tag{5.24}$$

where $\alpha\tilde{p}$ denotes pressure increase due to the vortical layer. Substituting Eqs. (2.3), (2.5), (5.17), (5.21) and (5.24) into Eq. (5.23) and neglecting the terms of order of α^2, then, leads to

$$\left.\begin{aligned}&\tilde{p}=\frac{S_1}{(\gamma-1)c_v}\,\omega_0F^{\gamma}(\xi_c),\\ &\zeta=1+\frac{S_1}{2\tau^2\gamma c_v}\,\frac{1+\dfrac{2}{(\gamma-1)M^2}-(1+\tau^2\xi_c^{\,2})(\tilde{a}+\tau^2u_{0c})^2}{(1+\tau^2\xi_c^{\,2})(\tilde{a}+\tau^2u_{0c})u_{1e}}.\end{aligned}\right\} \tag{5.25}$$

Now that ζ is known, correct distribution of velocity at cone surface can be obtained from Eqs. (5.20) and (5.21), and density distribution is given by the equation

$$p_c=(\omega_0-\alpha\omega_1)\rho_c^{\,\gamma},$$

which can be simplified by neglecting the terms of order of α^2 as

$$\rho_c=\rho_{0c}\left\{1+\alpha\left(\frac{1}{\gamma-1}\,\frac{S_1}{c_v}+\frac{1}{\gamma}\,\frac{p_{1e}}{p_{0c}}\sin\theta\right)\right\}. \tag{5.26}$$

6. Results and Discussions

Since the unknown constant κ is involved in shock wave conditions appropriate to perturbation field due to angle of attack, integration of Eq. (4.8) must be carried out, by use of a trial and error method, by assuming initially several values of κ, finding out a proper value satisfying Eq. (5.22). The actual calculation was carried out by use of a HIPAC 5020 digital computer and the results are tabulated in Table 1.

TABLE 1.

M	$\delta^{(\circ)}$	τ	p_0	p_1	κ	ζ
2	8	0.5938	0.6213	−0.7712	2.142	1.0120
	16	0.6886	0.6110	−1.0788	1.170	0.9775
	24	0.8878	0.5076	−0.8951	0.615	0.8906
	32	1.2218	0.3619	−0.5674	0.260	0.7845
3	8	0.3779	0.7706	−1.9165	2.230	1.0051
	16	0.4910	0.7334	−2.1471	0.860	0.8909
	24	0.6619	0.6270	−1.6538	0.346	0.7325
	32	0.9036	0.4919	−1.0706	0.100	0.5899
4	8	0.2938	0.8309	−3.1518	2.130	0.9801
	16	0.4193	0.7699	−2.9635	0.620	0.7784
	24	0.5914	0.6623	−2.1040	0.182	0.6011
	32	0.8156	0.5328	−1.3334	0.005	0.4964

Aerodynamic coefficients for a circular-cone are defined by the equations

$$\left.\begin{aligned} Cn_\alpha &= -\frac{\tau^2}{\tan\delta}\, p_{1e}(\xi_c)\,, \\ Cx_0 &= 2\tau^2 p_0(\xi_c)\,, \\ Cm_\alpha &= -\frac{2}{3}\tau^2\,\frac{1+\tan^2\delta}{\tan\delta}\, p_{1e}(\xi_c)\,, \\ \bar{x}_{c.p} &= \frac{2}{3}(1+\tan^2\delta)\,, \end{aligned}\right\} \tag{6.1}$$

where Cx_0 denotes axial force coefficient at zero angle of attack and Cm is defined as pitching-moment coefficient round the nose and head-down moment is taken to be positive.

Figs. 2 to 4 show variations of aerodynamic coefficients with semi-vertex angle for Mach numbers of 2, 3 and 4, respectively. For any Mach number, slope of normal force coefficient decreases monotonously with increase of δ, indicating that it depends mainly upon semi-vertex angle but is less sensitive to Mach number. The same trend has already been confirmed by Buford [12] experimentally by use of a circular-cone with $\delta=10°$. In order to compare the present theory with the others, data of Cn_α obtained from Sim's table [5] are also plotted in these figures. It is found from the figures that there exists a fairly large difference between present results and Sims' data near $\delta=10°$, beyond which the difference is minimized. The reason for this is not clear.

Cm_α seems to depend strongly upon Mach number, since its behaviour is quite different from each other for various Mach numbers, as is seen in the figures. In particular, it is remarkable that Cm_α at $M=4$ changes from decreasing to increasing as cone angle grows. Since both Cn_α and Cm_α obtained from the present theory have a trend to agree with linearized theory in the limiting case when cone angle

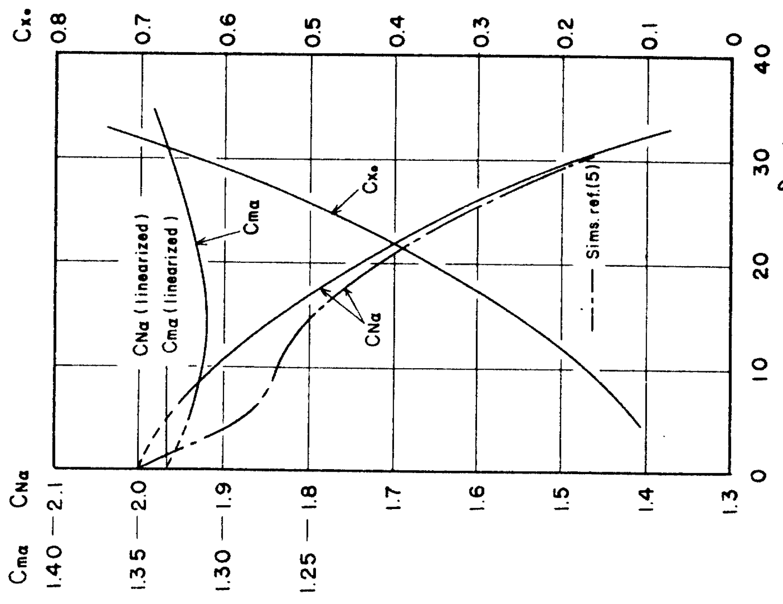

FIG. 2. Variation of Cn_α, Cm_α and Cx_0 with semi-vertex angle of cone. $M=2$.

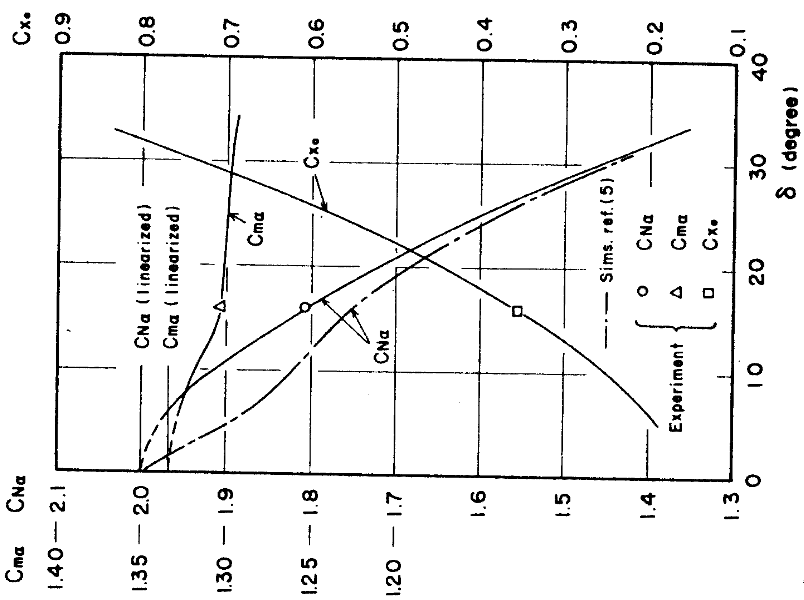

FIG. 3. Variation of Cn_α, Cm_α and Cx_0 with semi-vertex angle of cone. $M=3$.

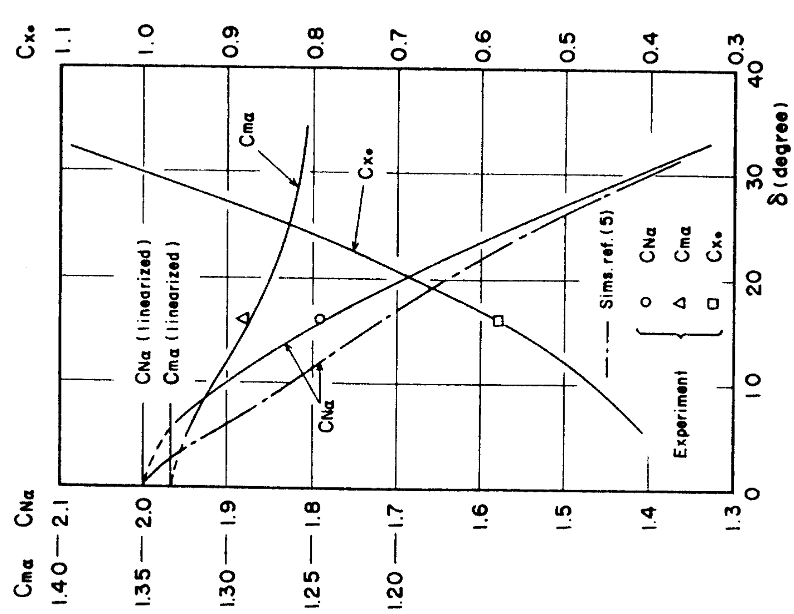

FIG. 4. Variation of Cn_α, Cm_α and Cx_0 with semi-vertex angle of cone. $M=4$.

tends to vanish, deviation from the linearized theory indicates nonlinear effects of the fundamental equations on aerodynamic characteristics of a lifting cone at supersonic speeds.

Fig. 5 shows variation of location of center of pressure with semi-vertex angle. For circular-cones the location of center of pressure depends only upon cone angle and it moves backwards monotonously as cone angle increases. Moreover, it is noticeable that it retires away from base of the cone as growing cone angle goes beyond 35.26°. Although this result may seem to be curious at a glance, it is really reasonable from the fact that axial component of surface pressure has a fairly large amount of contribution to pitching moment round the nose.

In Fig. 6 is presented variation of κ with semi-vertex angle for various Mach numbers together with Sims' data for comparison. As is seen in the figure, κ decreases monotonously with increase of cone angle. This trend clearly confirms a physical fact that, the more the body becomes blunt, shock wave shape is less sensitive to body shape. Moreover, it may be an interesting result that, at $M=4$ and $\delta=32°$, shock wave shape relative to the cone at small angles of attack is almost unchanged from that at zero angle of attack, while surface pressure changes greatly. This may be due to a strong effect of cross flow. In reference [5] are presented values of ratio of shock wave yaw, η, to body yaw, α, so that a simple

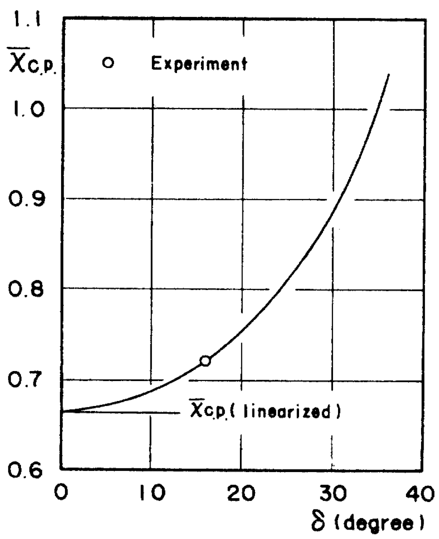

FIG. 5. Location of center of pressure for cone.

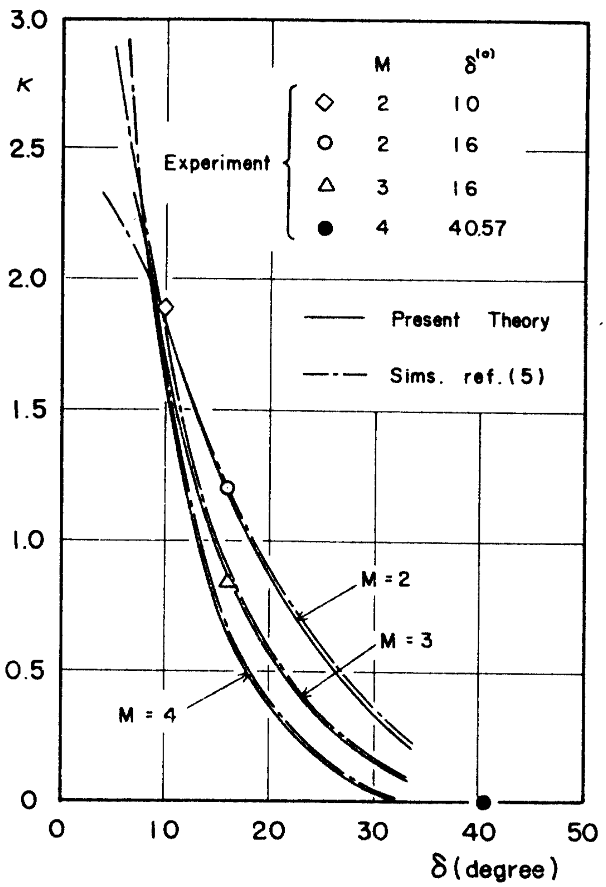

FIG. 6. Variation of κ with semi-vertex angle of cone.

transformation relation obtained by neglecting the terms of order of α^2 was used for interpretation of Sims' data, which is expressed as

$$\kappa=\frac{1+\tau^2}{\tau}\left(1-\frac{\eta}{\alpha}\right) \tag{6.2}$$

So long as κ is concerned, the agreement between present theory and Sims' data is quite good, as is seen in the figure.

7. Experiment

As has been already pointed out in the last section, there exists a remarkable difference in behaviour of Cn_α between present theory and Sims' data. However, as to the other aerodynamic characteristics, for example, κ etc., any serious difference does not seem to exist and, therefore, an experimental confirmation on this point becomes of a primary interest.

In order to confirm the theoretical results obtained from present development an experimental investigation was carried out by use of a blow-down type supersonic wind tunnel. Two models made of steel were used in the experiment, the one is a finite cone with semi-vertex angle of 16° and the another is a cone-cylinder with semi-vertex angle of 40.57°. The former was used for measurement of aerodynamic forces and surface pressure distribution and the latter for schlieren observation only. Detail of size of the models is shown in Fig. 7. Reynolds number of model (A) referred to cone length is 2.73×10^6 at $M=2$ and 6.80×10^6 at $M=3$, respectively, and Reynolds number of model (B) referred to nose-cone length is 7.41×10^6 at $M=4$.

A sting balance of moment type with 22 mmϕ in diameter and 195 mm in length was used to measure normal, axial forces and pitching moment. Since a cylindrical afterbody may contribute to some extent to aerodynamic forces, the sting balance was used only for model (A). In this case, however, another difficulty arised in the measurement that almost over a half in length of the sting balance must be exposed in air stream at high speed, because the model was shorter. In order to avoid this difficulty a cylindrical steel pipe of 30 mmϕ in outer diameter was, as a protection, so used not to interfere with the balance. Moreover, model (A) has 8 holes at its base in order to measure an average value of base pressure.

Figs. 8 and 9 show measured surface pressure distribution on model (A) at Mach numbers of 2 and 3, respectively, together with theoretical results for comparison. Agreement between theory and experiment is fairly good. In Figs. 10 and 11 are presented variations of measured aerodynamic characteristics with angle of attack. In the figures, axial force coefficient, Cx, is defined by the equation

$$Cx=Cx_T+Cx_B, \tag{7.1}$$

where Cx_T and Cx_B denote total coefficient measured by the balance and thrust coefficient due to base pressure, respectively. Axial force coefficient due to skin friction is neglected in experimental evaluation of Cx, since, from a theoretical evaluation, it is found to be very small compared with the others.

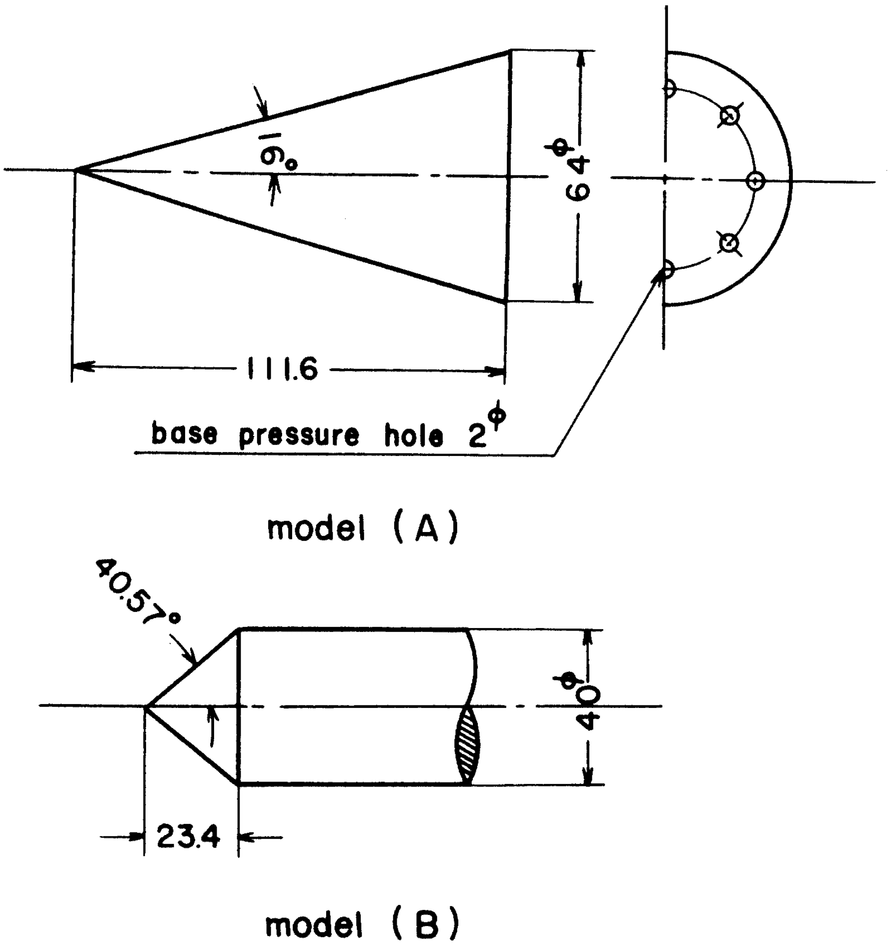

FIG. 7. Models.

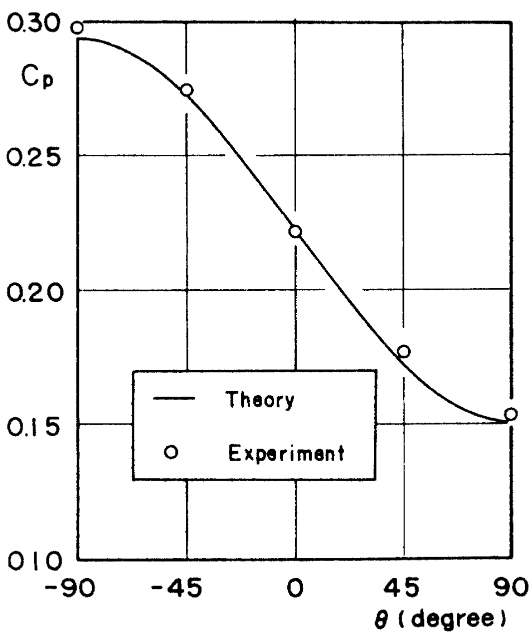

FIG. 8. Surface pressure distribution on cone. $M=2$, $\alpha=4°$.

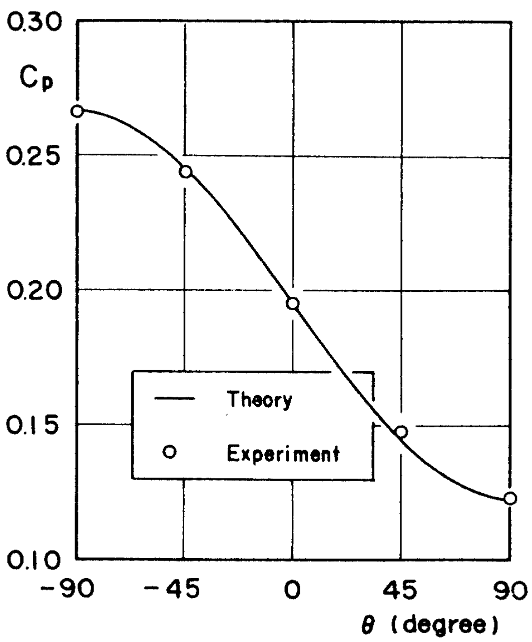

FIG. 9. Surface pressure distribution on cone. $M=3$, $\alpha=4°$.

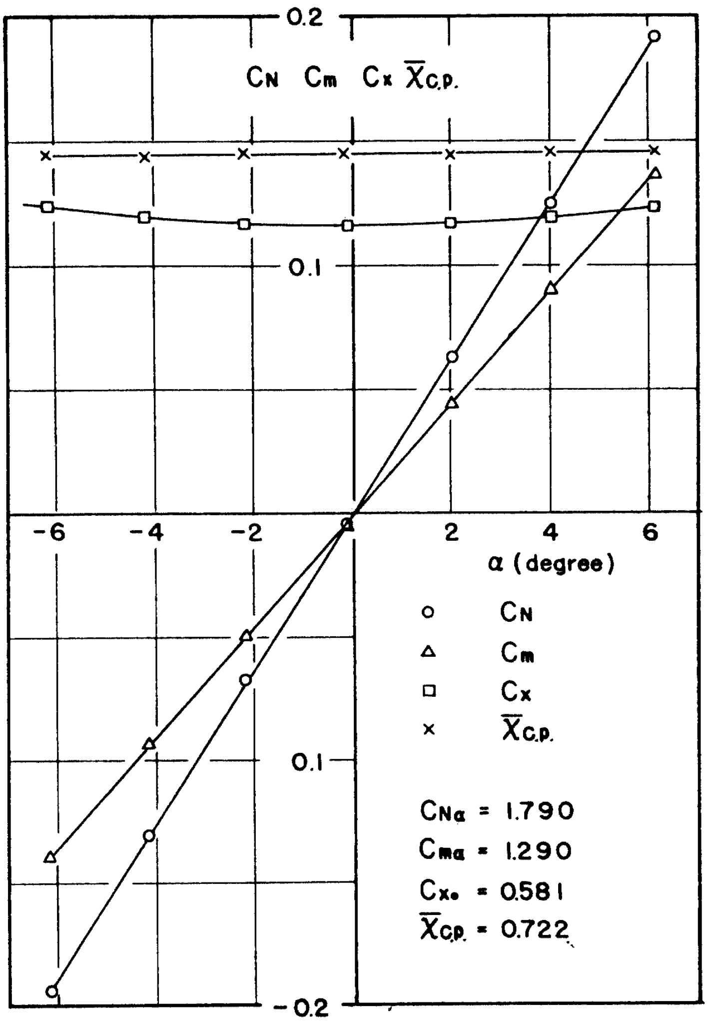

FIG. 10. Variation of Cn, Cm, Cx and $x_{c \cdot p}$ with angle of attack. $M=2$.

As is seen in the figures, both normal force and pitching-moment coefficients vary linearly with angle of attack up to $\pm 6°$, thus confirming the linear approximation of perturbation properties with respect to small angles of attack. The same linear variation of normal force and pitching-moment was shown by Hottner [*13*] experimentally, using a circular-cone with $\delta=10°$ mounted in a shock tunnel at $M=3.86$. Experimental slopes of normal force and pitching-moment coefficients and axial force coefficient at zero angle of attack are also plotted in Figs. 2 and 3 and location of center of pressure is plotted in Fig. 5 for comparison. As is seen in the figures, the agreement between theory and experiment is quite good.

In order to further confirm the present theory, a schlieren observation of shock wave attached to model (A) was made for Mach numbers of 2 and 3. Several photographs are shown in Figs. (12a) to (12d). Values of κ obtained from schlieren photographs are plotted also in Fig. 6 together with another datum at $M=2$ and $\delta=10°$ for comparison. Furthermore, a schlieren observation of shock wave shape was made for a Mach number of 4 by use of model (B). This model

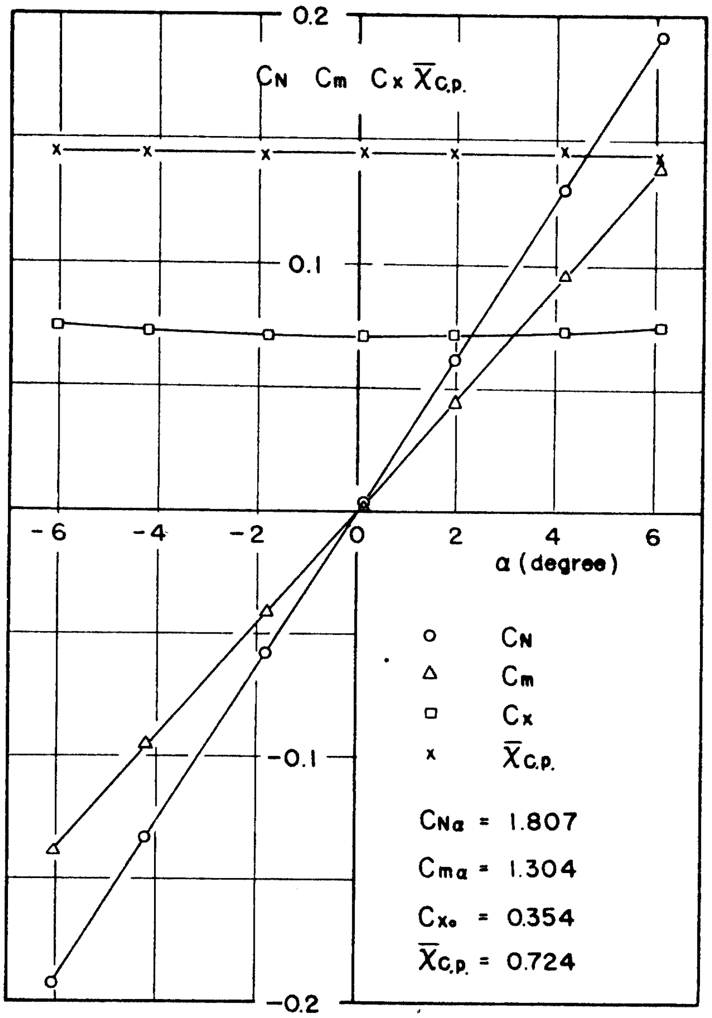

FIG. 11. Variation of Cn, Cm, Cx and $x_{c \cdot p}$ with angle of attack. $M=3$.

has a fairly large semi-vertex angle than 32° at which the present theory reveals that shock wave shape relative to the body is almost insensitive to small angles of attack, when $M=4$. Furthermore, at semi-vertex angle of model (B), Sims' data seem to indicate that relative location of shock wave axis to body axis will be reversed at $M=4$. Figs. (13a) and (13b) show schlieren photographs of flow pattern past model (B) at $\alpha=0°$, $M=4$ and $\alpha=4°$, $M=4$, respectively. The figures clearly show that the shock wave shape relative to the cone at $\alpha=4°$ is almost unchanged from that at zero angle of attack. However, the deduction of reversion of relative location of shock wave axis to body axis mentioned above cannot be confirmed obviously from these figures.

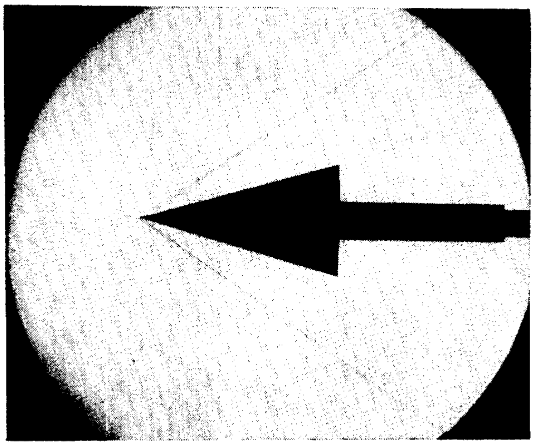

FIG. 12a. Schlieren photograph of a flow field around a cone. $M=2$, $\delta=16°$, $\alpha=0°$.

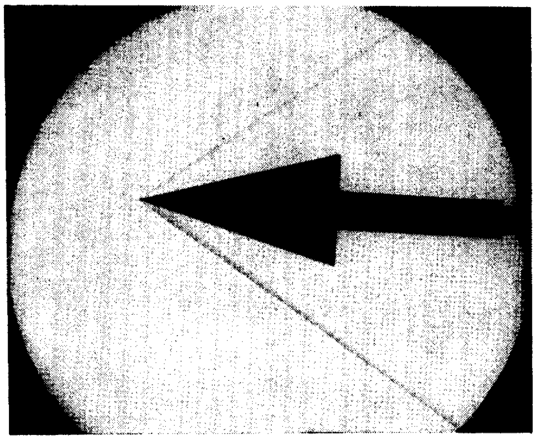

FIG. 12b. Schlieren photograph of a flow field around a cone. $M=2$, $\delta=16°$, $\alpha=4°$.

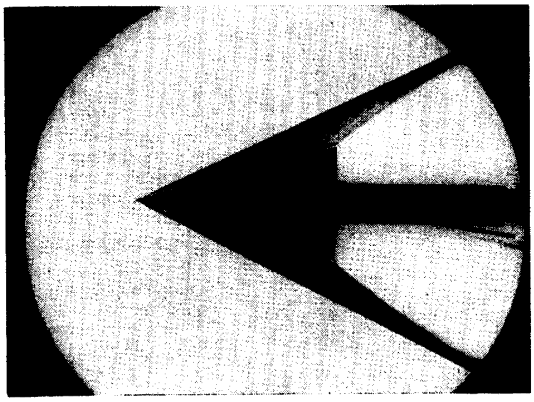

FIG. 12c. Schlieren photograph of a flow field around a cone. $M=3$, $\delta=16°$, $\alpha=0°$.

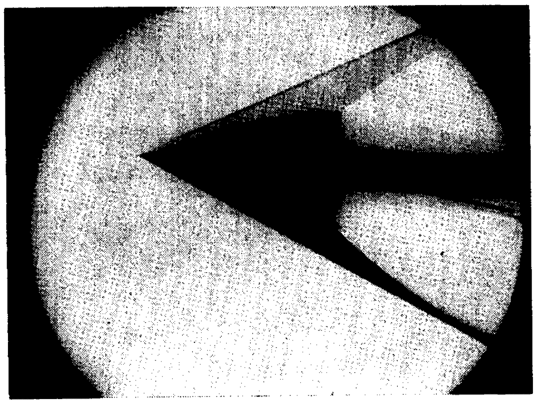

FIG. 12d. Schlieren photograph of a flow field around a cone. $M=3$, $\delta=16°$, $\alpha=4°$.

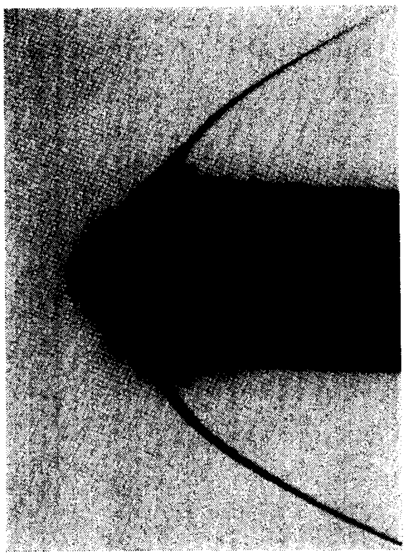

FIG. 13a. Schlieren photograph of a flow field around a cone. $M=4$, $\delta=40.57°$, $\alpha=0°$.

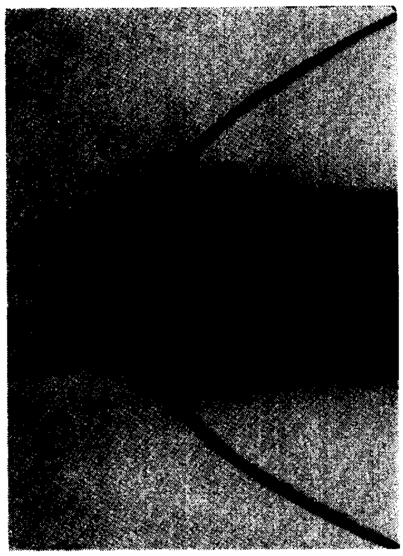

FIG. 13b. Schlieren photograph of a flow field around a cone. $M=4$, $\delta=40.57°$, $\alpha=4°$.

8. Conclusion

A general method of analytical approach to supersonic flow past pointed bodies of revolution at small angles of attack was presented and applied to circular-cones as a simple example. It is shown that nonlinearity in fundamental equations has predominant effects on aerodynamic characteristics of lifting bodies, thus indicating that the linearizezd theory does not adequately predict an essential feature of flow phenomena.

However, it is noticeable that a linear approximation of lifting flow field with respect to small angles of attack is still available even if the body is not so slender for which an essential feature of the basic flow field is nonlinear. This fact was also confirmed by the present experiment.

The assumptions used in the present development and also in works of Stone and Ferri was shown to be consistent essentially with an assumption of isentropic flow everywhere in the disturbed field which causes a discontinuous distribution of entropy near the body surface. This difficulty, however, was shown to be avoidable, if body thickness is small. Furthermore, even in case that the body is not so slender, the present development was shown to be applicable by introducing a simple correction of entropy distribution near the surface.

The fact that a parameter κ, which corresponds to deviation of shock wave axis from body axis due to small angles of attack, decreases monotonously as cone angle grows clearly indicates a physical evidence that shock wave shape is less sensitive to body shape as the body becomes blunt.

Acknowledgement

The authors express their gratitude to Mr. M. Uchida and Mr. T. Hara at Mechanical Engineering Research Laboratory, Hitachi Ltd. for their kind cooperation in programming and computation by use of a HIPAC 5020 digital computer.

Department of Aerodynamics,
Institute of Space and Aeronautical Science,
University of Tokyo, Tokyo
June 25, 1966

References

[1] Taylor, G. I. and Maccoll, J. W.: The Air Pressure Over a Cone Moving at High Speeds. Proc. Roy. Soc. (London), A, Vol. 139, No. 838, 1933.

[2] Stone, A. H.: On Supersonic Flow Past a Slightly Yawing Cone. Jour. Math. and Phys., Vol. 27, No. 1, 1948.

[3] Staff of the Computing Section, Center of Analysis: Tables of Supersonic Flow Around Yawing Cones. Tech. Rep. 3, MIT, Cambridge, Mass., 1947.

[4] Ferri, A.: Supersonic Flow Around Circular Cones at Angles of Attack. NACA TN 2236, 1950.

[5] Sims, J. J.: Tables for Supersonic Flow Around Right Circular Cones at Small Angle of Attack. NASA SP-3007, 1964.

[6] Ferri, A.: The Method of Characteristics for the Determining of Supersonic Flow Over Bodies of Revolution at Small Angles of Attack. NACA Rep. 1044, 1951.

[7] Ferri, A.: The Linearized Characteristics Method and Its Application to Practical Nonlinear Supersonic Problems. NACA Rep. 1102, 1952.

[8] Ferri, A.: Linearized Characteristics Methods. Ch. 6, sec. G of General Theory of High Speed Aerodynamics. Priceton, 1954.

[9] Rakich, J. V.: Numerical Calculation of Supersonic Flows of a Perfect Gas Over Bodies of Revolution at Small Angles of Yaw. NASA TN D-2390, 1964.

[10] Van Dyke, M. D. and Gordon, H. D.: Supersonic Flow Past a Family of Blunt Axisymmetric Bodies. NASA TR R-1, 1959.

[11] Karashima, K.: The Flow Near the Region of Vertex of Axially Symmetric Bodies at Supersonic Speeds. Inst. Space and Aero. Sci. Univ. Tokyo, Rep. No. 400, 1966.

[12] Buford, W. E.: The Effects of Afterbody Length and Mach Number on the Normal Force and Center of Pressure of Conical and Ogival Nose Bodies. Jour. Aero Sci. Feb., 1958.

[13] Hottner, T.: Untersuchungen an einem Modell-Rohrwindkanal bei Machzahlen von Ma = 3 bis 6. Zeitschrift für Flugwissenschaften 13. Jahrgang, Heft 7, July, 1965.